Available online at www.sciencedirect.com

ScienceDirect

Procedia Manufacturing 18 (2018) 97–103

Procedia MANUFACTURING

www.elsevier.com/locate/procedia

18th Machining Innovations Conference for Aerospace Industry, MIC 2018

Surface texturing of TiAl6V4 using cutting tools in reverse

Eric Segebade[a]*, Daniel Kümmel[b], Frederik Zanger[a], Johannes Schneider[b], Volker Schulze[a]

[a] *wbk Institute of Production Science, Karlsruhe Institute of Technology (KIT)*
[b] *IAM Institute for Applied Materials, Karlsruhe Institute of Technology (KIT) and MicroTribology Center µTC*

Abstract

The usability of Ti-alloys in tribological systems is limited due to high wear rates during sliding. Therefore, many parts of critical aircraft assemblies are built using steel instead. Empowering Ti-alloys to be used in tribological systems will therefore enable a significant reduction of weight in e.g. landing gears. Surface texturing is widely used to improve the tribological behavior of metal parts. Most texturing methods using cutting tools depend on chip formation as the primary mechanism of texturing. In this work, a chipless process of surface texturing titanium parts using a cutting tool is developed. To this end, the resulting texture geometry variance is analyzed regarding the process parameters. It could be demonstrated in selected tribological experiments, that the textured surfaces produced using the chipless process are far superior to textures produced by chip formation.

Peer-review under responsibility of the scientific committee of the 18th Machining Innovations Conference for Aerospace Industry.

Keywords: Type your keywords here, separated by semicolons ;

1. Introduction

Wear behavior of Ti-alloys is limiting its use in tribological applications. Particularly its strong adhesive wear, an unstable and rather high coefficient of friction (COF), as well as sensitivity to fretting wear are adverse [1]. This behavior can in part be attributed to shear-banding behavior of Ti-alloys [2]. Usual methods to enhance the friction and wear behavior of Ti-alloys are coating [3] and surface texturing [4] or combinations thereof [5]. Advanced surface

a wbk Institute of Production Science, Karlsruhe Institute of Technology (KIT)
b IAM Institute for Applied Materials, Karlsruhe Institute of Technology (KIT) and MicroTribology Center µTC
* Corresponding author. Tel.: +49-721-608-45906; fax: +49-721-608-45004.
E-mail address: eric.segebade@kit.edu

2351-9789
Peer-review under responsibility of the scientific committee of the 18th Machining Innovations Conference for Aerospace Industry.
10.1016/j.promfg.2018.11.013

texturing processes include the use of lasers [6, 7], or machining operations like turn-milling [8] and vibration assisted machining [9]. The aim of surface texturing can be both, increasing [10] and lowering [11] the COF. In general, machining based texturing methods rely on the removal of material [8-9, 12-13].

In several technical applications, there is a multitude of moving parts, which are in dynamic or near-static contact and could be manufactured from Titanium alloy considering the mechanical loads present. However, Titanium consistently fails to be eligible for most of these due to its unfavorable wear behavior. Thus, new methods to enhance friction and wear behavior of Titanium-alloys are of high interest.

In this work, a new method of texturing TiAl6V4 surfaces using commercial cutting inserts directly after face turning without chip formation is developed. An experimental study of process parameters comprised of texturing depth (at), and texturing speed (vt) yields first knowledge of the resulting texture geometry for a range of process parameters. The process of Complementary Texturing (CT) is inspired by laser-created groove-textures with adjacent recast material, and similar to the process strategy Complementary Machining (CM) [14,15]. Pin-on-disc experiments were used to compare textures based on regular cutting with those produced by CT and an as-machined reference.

2. Experimental and analytical setup

Experiments were conducted using TiAl6V4 round bars with Ø 50 mm. Uncoated DNMG 150612 inserts from Walter Tools with a nominal edge radius $r_\beta = 40$ µm were used for face turning on an Index V100 vertical turning center. The machine tool features a fixed tool with the rotating spindle moving on three axes. All samples were subjected to a pre-cut of 0.1 mm depth at 0.1 mm/rev feed and 160 m/min cutting speed in lubricated condition. The respective texture was applied by using the tool in the opposite direction analogous to CM. In CM, the workpiece is first machined regularly (Fig. 1 a). Afterwards, the tool is moved along the surface in the opposite direction, introducing plastic deformation to the surface layer (Fig. 1 b). Analogous to this, CT is comprised of a standard finish-turning process and a subsequent usage of the tool in the opposite direction using a small texturing depth to inhibit chip formation. While the main goal of CM is the enhancement of surface layer states, CT aims for a specific type of groove texture, which consists of a groove flanked by burrs.

Specimens with textures applied using the spindle rotation resulted in spirals (Fig. 2 a). For a basic analysis of how chip formation differs from CT at extreme parameters, two such spirals were produced. Using a very low cutting speed of $v_c = 0.1$ m/min at a depth of cut $a_p = 0.01$ mm the first spiral was cut ($f = 1.3$ mm/rev). In spite of the extremely low cutting speed and small cutting depth, chip formations ensured. The second spiral was produced by CT with a texturing speed of $v_t = 160$ m/min at a texturing depth of $d_t = 0.01$ mm ($f = 1.3$ mm/rev). No chip formation was observed during texturing of the second spiral.

The kinematics of pin-on-disc experiments concurrent with the desired investigation (grooves perpendicular to relative motion) required segmented specimens (Fig. 2 b). Therefore, specimens for the geometrical analysis as well as the pin-on-disc experiments were produced using the translational axes of the machine with a top speed of 30 m/min. For the geometrical analyses, segmented textures were produced according to the parameters listed in Table 1. All samples were analyzed optically with a confocal light microscope type Nanofocus µsurf regarding the measured texture height ($h_{t,m}$), width ($w_{t,m}$) and depth ($d_{t,m}$) at 11 equidistant positions along a groove track of 7 mm.

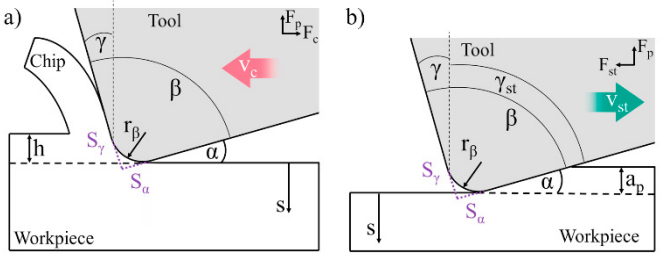

Fig. 1: Complementary Machining strategy [14]. Regular cutting a) followed by Complementary Machining b) without chip formation and reversed tool.

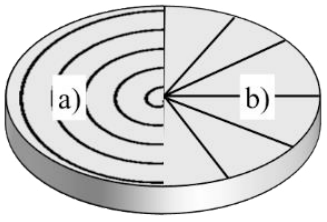

Fig. 2: a) concept drawing of spiral-specimen b) concept drawing of segmented specimen.

Table 1: Conducted experiments considering segmented specimens produced using varying speeds and depths.

Texturing speed v_t in m/min	Texturing depth d_t in µm
0.1 to 30	10
0.5	1 to 20

The textures produced for pin-on-disc experiments had a theoretical groove density of 50%. For comparison, specimens were produced using CT, and cutting. In both cases, a texturing/cutting speed of 0.5 m/min and a texturing depth/depth of cut of 0.01 mm was applied. Additionally, an as-machined sample served as reference (pre-cut condition). The unidirectional tribological test setup (Plint TE92 HS Tribometer) is shown in Fig. 3. The testing procedure comprised of decreasing velocity ramps is depicted in Fig. 4. Using a CuAl10Ni5Fe4 pin with a diameter of 8 mm as a counter body, a nominal pressure of 1 MPa was applied. This pressure was chosen to ensure occurence of the lubrication states from hydrodynamic to boundary lubrication in all samples. The first sliding velocity of 2.5 m/s was kept constant for 60 minutes. All other velocities were kept constant for 15 minutes each, finishing the experiment after 15 min of 0.1 m/s velocity and a total time of 210 min. The setup was lubricated using additive-free FVA 2 mineral reference oil. The total sliding distance per sample was 14.6 km. During the experiments, the linear displacement of the pin was recorded with an inductive sensor. The linear displacement of the pin corresponds to the cumulative linear wear during the experiment. It constitutes the sum of wear from both, pin and disc, without the possibility of discerning the two.

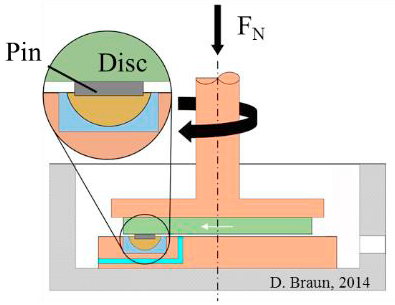

Fig. 3: Concept of the used Plint TE92 HS Tribometer [16]

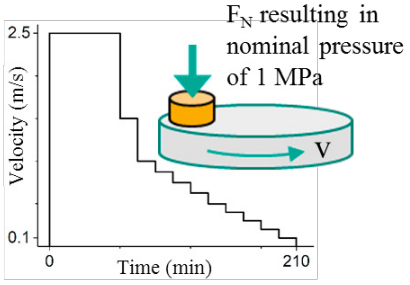

Fig. 4: Test regime based on decreasing velocity-ramps.

3. Results and discussion

An exemplary CT specimen produced at low speed is shown in Fig. 5. The burr formation during the process resulted in a high irregularity with regard to both, burr position and dimension. In Fig. 6, a SEM-image shows what could be identified as shear bands leading up to the burr. From both images it is clear, that the texture was created by material displacement rather than removal. This mechanism of texturing could not be reproduced by cutting a spiral at very low speed (v_c = 0.1 m/min) and cutting depth (a_p = 0.01 mm), as can be seen in Fig. 7, but still applies for CT of a spiral at high speed (v_t = 160 m/min, a_t = 0.01 mm) as shown in Fig. 8. Figures 7 a) and 8 a) show the measured topography and a contour height analysis. The latter shows clearly, that while in the cut spiral (Fig. 7) 25.6 % of the projected surface can be attributed to the grooves (blue), this value increases to 41.8 % for the spiral produced by CT (Fig. 8). Additionally, 17.9 % of the projected surface was attributed to the burrs formed by CT (red). In both cases the height range of the bulk material was spanning some 5 µm. Both measurements were corrected regarding outliers and measurement errors before analysis by determining the smoothed mean of neighbors. Figures 7 b) and 8 b) show exemplary profiles through the texture. Values written within the figures represent mean values and standard deviations of all complete grooves captured over the whole measurement area of 0.8 by 10 mm. The mean depth, height and width were measured using the mean height of the surface excluding the textured areas, ensuring a common baseline across measurements. In both cases, the measured depth reflects the desired texturing depth within a

reasonable deviation. Calculating the theoretical width for a depth of 10 µm (considering the tool geometry and disregarding elasticity) suggests a width of 309 µm.

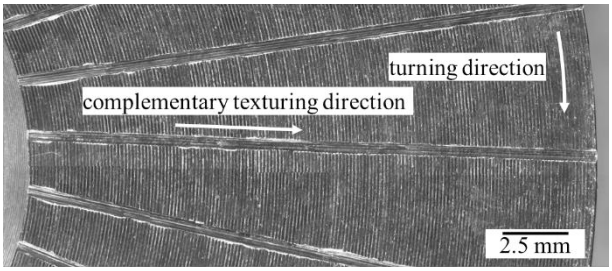

Fig. 5: Example of a segmented specimen with processing directions.

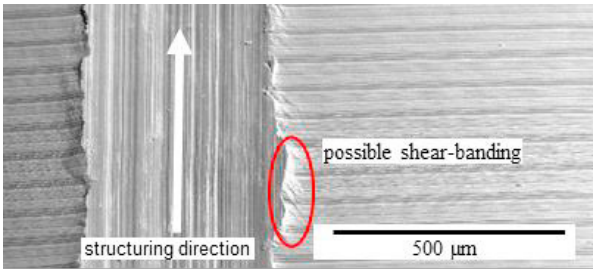

Fig. 6: SEM-image of a groove, shear-banding area highlighted.

This does not correspond to the width of either sample. While the cut sample features a width of 344 ± 15 µm, the CT sample shows a groove width of 430 ± 28 µm. This is reflected in the different projected areas of the grooves of both samples. A possible reason for the discrepancy of the measured and calculated width is adhesion and subsequent ploughing taking place during groove formation, which would also explain the smaller grooves on the bottom of the primary groove. The maximum burr height of the CT sample in the analyzed area was 22 µm (mean value of 13.8 ± 3.9 µm). Across the sample, burr height and width varied significantly. This could either be attributed to the interaction with the surface roughness or to shear-banding of the material leading to variances of the direction of material displacement. Burr formation was not observed on the cut sample.

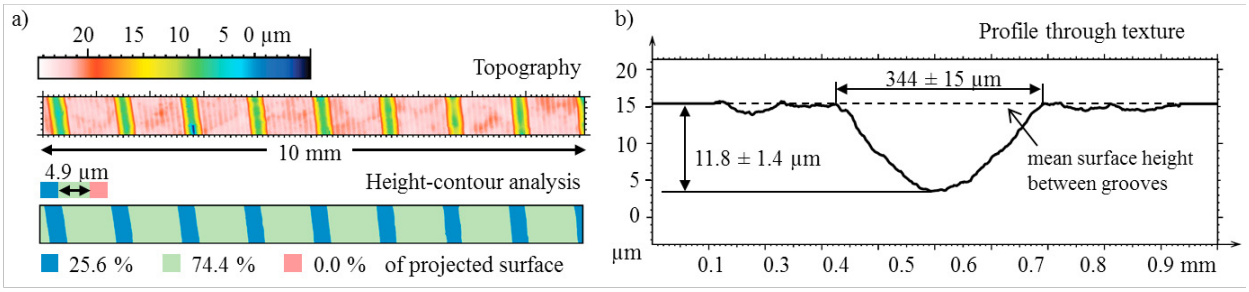

Fig. 7: Cut spiral at v_c = 0.1 m/min; a_p = 0.01 mm; f = 1.3 mm/rev. a) topography and height contour analysis, b) profile of texture including mean values of measured width and depth.

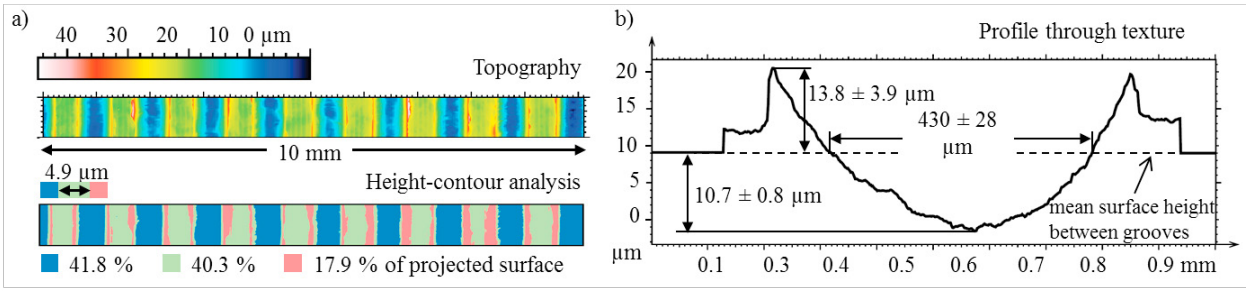

Fig. 8: Chipless textured spiral at v_t = 160 m/min; d_t = 0.01 mm; f = 1.3 mm/rev. a) topography and height contour analysis, b) profile through texture including mean values of measured width, height and depth.

The result of the measured width ($w_{t,m}$) concurrent with the measured depth ($d_{t,m}$) of the segmented specimens (Fig. 2 b) is shown in Fig. 9. For reference, the texturing depth (d_t) and resulting theoretical width ($w_{t,t}$) are also shown. Fig. 10 shows the measured height ($h_{t,m}$) and depth ($d_{t,m}$) versus d_t. The measured width $w_{t,m}$ corresponds well to the

theoretical width $w_{t,t}$, considering the measured depth $d_{t,m}$ rather than the texturing depth d_t. However, a large discrepancy between the texturing depth d_t and the measured depth $d_{t,m}$ is apparent (Fig. 10).

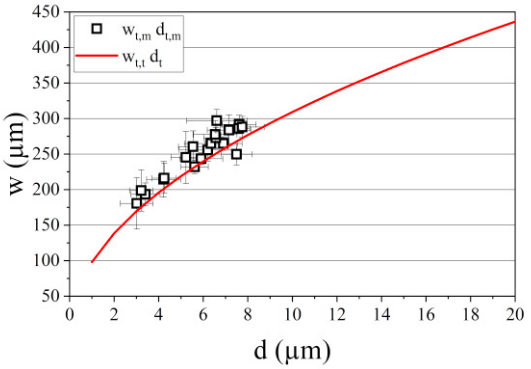

Fig. 9: Width (w) versus depth (d) of segmented specimens at v_t = 0.5 m/min.

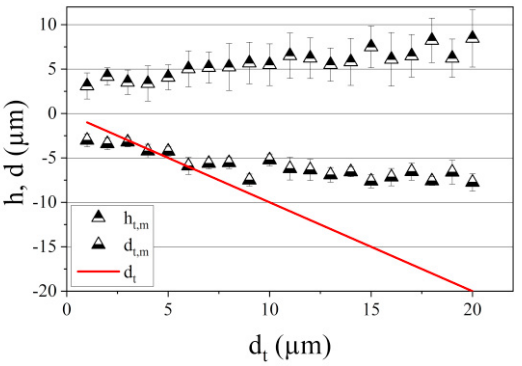

Fig. 10: Measured height (h) and depth (d) versus texturing depth (d_t) of segmented specimens at v_t = 0.5 m/min.

It is not clear, why $d_{t,m}$ does not scale to d_t, as the accuracy of the machine tool should lead to results at least close to the set parameters. The increase of $d_{t,m}$ at low speed on segmented specimens corresponds roughly to 0.2 times the increase in d_t. This also results in the discrepancy between the theoretical width $w_{t,t}$ and the measured width $w_{t,m}$ at any given texturing depth d_t.

Regarding the speed, a slight increase in width ($w_{t,m}$, see Fig. 11) and depth ($d_{t,m}$, see Fig. 12) towards the theoretical value of the texturing depth (d_t = 0.01 mm for all speeds) is observable. In the range of $30 < v_t < 160$ m/min, a sharp increase in width, depth and height of the resulting texture is observable. The identification of a possible transitional speed in this range will require further investigations, which may also increase understanding of the texture formation regarding its accuracy as well as its variance. All values shown were measured utilizing the mean surface height between grooves as shown in Figures 7 and 8.

It is possible, that the discrepancies result from tool deflection combined with adhesive ploughing and shear banding. Considering the comparable accuracy of the cut and CT spirals, the inaccuracy of the segmented specimens might also be attributable to the different kinematic involved. Further investigations are needed, especially to identify relations with higher speeds and tool geometries as well as the difference in influencing factors on the production of segments and spirals.

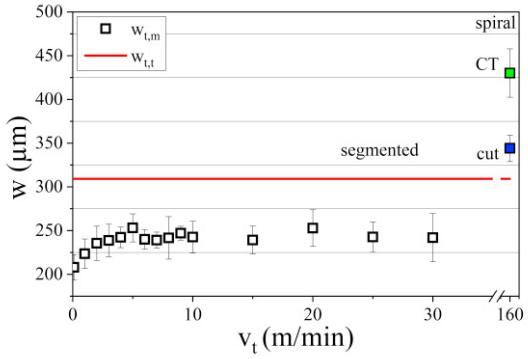

Fig. 11: Width (w) versus speed (v) of CT segmented specimens, and cut (blue) and (CT ,green) spirals at d_t = 10 µm ($w_{t,t}$ =309 µm).

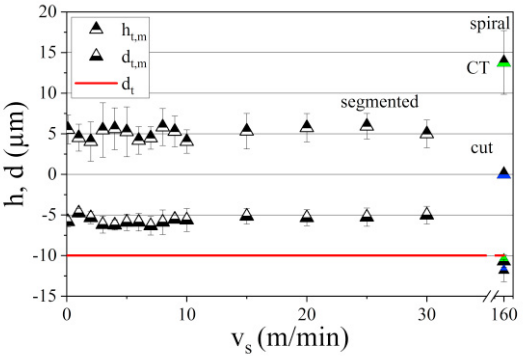

Fig. 12: Height (h) and depth (d) versus speed (v) of CT segmented specimens, and cut (blue) and (CT ,green) spirals at d_t = 10 µm.

The results of the tribological analysis are shown in Figures 13 and 14. The as-machined sample (black) exhibits a classic unsteady COF (Fig. 13), which changes from hydrodynamic friction to unsteady boundary lubricated friction between 0.5 and 0.4 m/s. The disc starts wearing out rapidly after 150 min of testing time, ending the experiment with

around 30 µm of linear wear (Fig. 14). In spite of the cut and CT texture featuring the same theoretical groove density of 50 %, the friction and wear behavior is quite different. The sample with the cut texture (red) shows a transition to boundary lubricated friction between 2 and 1 m/s. Even though the COF of the sample featuring the cut texture is in the same range as the as-machined one, it shows a constant high wear rate after 75 minutes, ending the experiment with a linear wear of close to 150 µm.

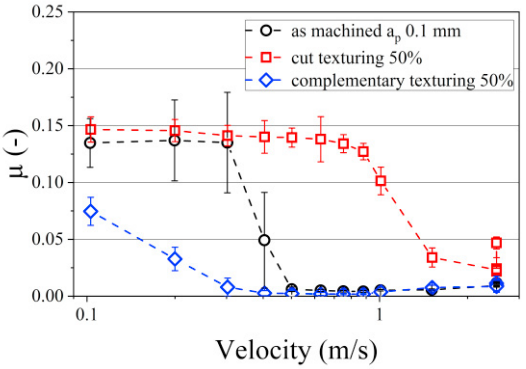

Fig. 13: Results of the tribological analysis, COF versus speed.

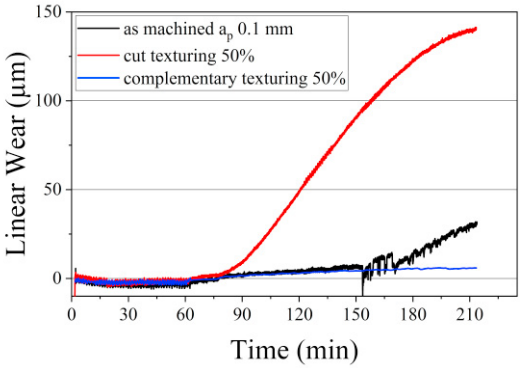

Fig. 14: Results of the tribological analysis, linear wear versus time.

In contrast to these two samples, the complementary textured sample behaves more favourable. Regarding the COF, the transition from fluid to sliding friction is much more gradual and starts at a low speed of 0.3 m/min. The linear wear at the end of the experiment is roughly 7 µm. In both textured cases, most of the wear can be attributed to the pin, since the textures are still visible after the experiments. A remnant of the burrs was still visible after the experiments, as can be seen in Fig. 15. In contrast to the nominal partial flat-on-flat contact of the cut sample, the burrs and possibly enhanced surface layer states thus result in a major difference in contact conditions leading to the enhanced friction and wear behavior under the conditions investigated in this work.

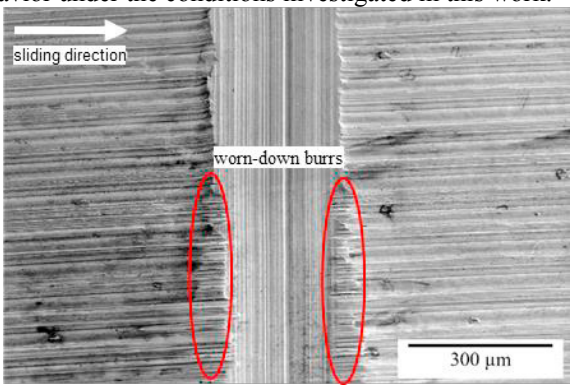

Fig. 15: Worn specimen with remaining complementary textured groove and worn burr. A residual burr height is still visible.

4. Summary and outlook

The alloy TiAl6V4 exhibits an undesirable tribological behavior, which can be enhanced by various methods. In this work, the Complementary Texturing (CT) method was developed and analyzed with regard to how the geometry of the textures is influenced by the process parameters texturing speed (v_t) and depth (d_t). While lower speeds do not change the resulting geometrical features (width, depth, height) significantly, a transitional speed resulting in a severe increase of the feature size was identified between 30 and 160 m/min. The set texturing depth did not correspond well to the measured depth at low speeds, and capped at around 9 µm using a texturing depth of 20 µm. Still, the relation of measured depth to measured width corresponded well will the theoretical width, calculated purely geometrically.

TiAl6V4 specimens were then used in pin-on-disc experiments. Compared to an untextured reference as well as a texture applied by cutting, the CT texture shows a significantly lower coefficient of friction (COF) during the whole experiment. Additionally, the cumulative linear wear measured during the experiment was much smaller than both, the reference and the cut texture. In the case of the textured samples, most of the wear was attributable to the pin rather than the disc. We can thus conclude, that the influence of using CT to apply a texture to a surface area adds more than a lubrication function, which should be achieved using a similar, cut texture. The possible tribological applications regarding pressures and speeds need to be investigated further.

Future work will focus on finding the transitional speed, quantifying the regularity of the textures and identifying a correlation of process parameters to desired texture geometry, also considering the interaction of the texturing process with the preceding cutting operation as well as optimization of the setup. Additionally, the wear behavior of more CT textures will be analyzed in order to identify the underlying wear mechanisms and identify an optimum with regard to textural features and density. This includes answering the question whether or not work hardening influences the tribological behavior of CT textures. Furthermore, measurement of processing temperatures and forces will enhance understanding of the process considerably. This should also promote to investigate the tool wear induced by this process, and therefore to assure, that the geometry of the tool remains constant.

Acknowledgements

The authors would like to thank the German BMWi for funding the experimental and analytical work within the scope of the project FAWIBO (20Y1505C), headed by Liebherr Aerospace.

References

[1] Budinski KG:Tribological properties of titanium alloys.In Wear 1991;151(2):203–17.
[2] Kailas SV, Biswas SK: The role of strain rate respinse in plane strain abrasion of metals. In Wear 1995;181-183(2):648-657.
[3] Pawlak W, Kubiak KJ, Wendler BG, Mathia TG: Wear resistant multilayer nanocompoite WC1-x/C coating on Ti-6Al-4V titanium alloy. In Tribology International 2015;82:400-406.
[4] Tian H, Saka N, Suh NP: Boundary Lubrication Studies on Undulated Titanium Surfaces. In Tribology Transactions 2004;32(3):289-296.
[5] He D, Zheng S, Pu J, Zhang G, Hu L: Improving tribological properties of titanium alloys by combining laser surface texturing and diamond-like carbon film. In Tribology International 2015;82:20-27.
[6] Ahui-Torres JI, Arenas MA, Perrie W, Demborenia J de: Influence of laster parameters in surface texturing of Ti6Al4V and AA2024-T3 alloys. In Optics and Lasers in Engineering 2018 103:100-109.
[7] Vorobyev AY, Gui C: Femtosecond laser structuring of titanium implants. In Applied Surfrace Science 2007;253(17):7272-7280.
[8] Karpuschewski B, Döbberthin C, Risse K, Deters L: Analysis of the Textured Surface of Tangential Turn-Milling. In Materials Performance and Characterization 2017;6(2):182-194.
[9] Kurniawan R, Kiswanto G, Ko TJ: Surface roughness of tow-frequency elliptical vibration texturint (TFEVT) method for micro-dimple pattern process. In International Journal of Machine Tools & Manufacture 2017;116:77-96.
[10] Dunn A, Castensen JW, Wlodarczyk KL, Hansen EB, Gabsdyl J, Harrison PM, Shephard JD, Hand DP: Nanosecond laser texturing for high friction applications. In Optics and Lasers in Engineering 2014;62:9-16.
[11] Nakano M, Korenaga A, Kernaga A, Miyake K, Murakami T, Ando, Usami H, Sasaki S: Applying Micro-Texture to Cast Iron Surfaces to Reduce the Friction Coefficient Under Lubricated Conditions. In Tribological Letters 2007;28:131-137.
[12] Denkena B, Köhler J, Mörke T, Gümmer O: High-Performance Cutting of Micro Paterns. In Procedia CIRP 2012;1:144-149.
[13] Greco A, Raphaelson S, Ehmann K, Wang QJ, Lin C: Surface texturing of tribological surfaces using the virbomechanical texturing method. In Journal of manufacturing science and engineering 2009;131(6):061005.
[14] Zanger F, Gerstenmeyer M, Weule H: Identification of an optimal cutting edge microgeometry for Complementary Machining. In CIRP Annals - Manufacturing Technology 2017;66(1):81-84.
[15] Gerstenmeyer M; Zanger F; Schulze V: Influence of Complementary Machining on fatigue strength of AISI 4140. CIRP Annals - Manufacturing Technology 2018 https://doi.org/10.1016/j.cirp.2018.04.103.
[16] Braun D, Grainer C, Schneider J, Gumbsch P: Efficiency of laser surface texturing in the reduction of friction under mixed lubrication. In Tribology International 2014;77:142-147.